Received: 14 November 2018 | Revised: 31 January 2019 | Accepted: 2 February 2019

DOI: 10.1111/cas.13964

ORIGINAL ARTICLE

WILEY Cancer Science

IFN/STAT signaling controls tumorigenesis and the drug response in colorectal cancer

Mizuho Sakahara[1] | Takuya Okamoto[1,2] | Jun Oyanagi[1] | Hiroshi Takano[1] | Yasuko Natsume[1] | Hitomi Yamanaka[1] | Daisuke Kusama[1] | Mishio Fusejima[1] | Norio Tanaka[3] | Seiich Mori[3] | Hiroshi Kawachi[4] | Masashi Ueno[5] | Yoshiharu Sakai[2] | Tetsuo Noda[6] | Satoshi Nagayama[5] | Ryoji Yao[1]

[1]Department of Cell Biology, Cancer Institute, Japanese Foundation for Cancer Research, Tokyo, Japan

[2]Department of Surgery, Graduate School of Medicine, Kyoto University, Kyoto, Japan

[3]Project for Development of Innovative Research on Cancer Therapeutics, Cancer Precision Medical Center, Japanese Foundation for Cancer Research, Tokyo, Japan

[4]Department of Pathology, Cancer Institute, Japanese Foundation for Cancer Research, Tokyo, Japan

[5]Department of Gastroenterological Surgery, Cancer Institute Hospital, Japanese Foundation for Cancer Research, Tokyo, Japan

[6]Director's Room, Cancer Institute, Japanese Foundation for Cancer Research, Tokyo, Japan

Correspondence
Ryoji Yao, Department of Cell Biology, Cancer Institute, Japanese Foundation for Cancer Research, Tokyo, Japan.
Email: ryao@jfcr.or.jp

Present address
Jun Oyanagi, Internal Medicine III, Wakayama Medical University, Wakayama, Japan

Funding information
Japan Society for the Promotion of Science, Grant/Award Number: 16H06276-1, 16K14620, 17H063333 and 18H02684

Colorectal cancer (CRC) is caused by genetic alterations, and comprehensive sequence analyses have revealed the mutation landscapes. In addition to somatic changes, genetic variations are considered important factors contributing to tumor development; however, our knowledge on this subject is limited. Familial adenomatous polyposis coli (FAP) is an autosomal-dominant inherited disease caused by germline mutations in the adenomatous polyposis coli (APC) gene. FAP patients are classified into two major groups based on clinical manifestations: classical FAP (CFAP) and attenuated FAP (AFAP). In this study, we established 42 organoids from three CFAP patients and two AFAP patients. Comprehensive gene expression analysis demonstrated a close association between IFN/STAT signaling and the phenotypic features of FAP patients. Genetic disruption of Stat1 in the mouse model of FAP reduced tumor formation, demonstrating that the IFN/STAT pathway is causally associated with the tumor-forming potential of APC-deficient tumors. Mechanistically, STAT1 is downstream target of KRAS and is phosphorylated by its activating mutations. We found that enhanced IFN/STAT signaling in CFAP conferred resistance to MEK inhibitors. These findings reveal the crosstalk between RAS signaling and IFN/STAT signaling, which contributes to the tumor-forming potential and drug response. These results offer a rationale for targeting of IFN/STAT signaling and for the stratification of CRC patients.

KEYWORDS
colorectal neoplasm, genetic background, genome editing, interferons, organoids

Mizuho Sakahara, Takuya Okamoto and Jun Oyanagi contributed equally to this work.

1 | INTRODUCTION

In CRC development, inactivation of the APC gene often occurs as the initial event in development of preneoplastic asymptomatic lesions known as adenomatous polyps. The step-wise accumulation of genetic alterations confers a malignant phenotype that leads to carcinoma formation. Comprehensive sequence analysis has revealed the genomic landscapes of human cancer,[1] which support the notion that alterations in key pathways, including Wnt signaling and RAS signaling, play critical roles in the initiation and progression of CRC development. Recently, this model of CRC development was biologically validated by application of genome-editing technology to organoid culture derived from the human colon.[2,3]

FAP is an autosomal-dominant inherited disease caused by germline mutations in the APC gene.[4] The second hit causes adenomatous polyps, which recapitulates the initial event of sporadic CRC development. According to the number of polyps and the age of onset, two major phenotypes of classical FAP (CFAP) and attenuated FAP (AFAP) have been described. CFAP is characterized by the presence of hundreds to thousands of polyps. Approximately half of patients develop adenomas by 15 years of age and 95% by 35 years. AFAP patients exhibit a milder phenotype than CFAP, characterized by a smaller number of polyps, later onset of adenomas, and lower CRC risk, although clinical definition of AFAP is controversial, and precise diagnosis is often difficult. It has been reported that the phenotypic difference between CFAP and AFAP is correlated with the germline mutation profiles of APC genes,[5,6] but their biological significance has not been fully understood.

In this study, we established 42 organoids from five FAP patients. Multiple organoids derived from the same patients enable us to explore the effects of somatic mutations under isogenic conditions. Importantly, these structures also supply the opportunity to investigate the biological significance of individual genetic backgrounds by elucidating the differences in organoid sets derived from identical patients. In this work, we show that the attempt to identify the molecular basis of phenotypic differences between CFAP and AFAP reveals the outcomes of the genetic variation in tumor-formation potential and the response to chemotherapeutic agents.

2 | MATERIAL AND METHODS

2.1 | FAP organoid culture

FAP tumor samples were obtained from consenting patients, and all procedures were approved by the Research Ethics Board at the JFCR Cancer Institute (Tokyo, Japan). Following surgical resection, tumors were immediately cut into small pieces and washed with PBS. Tumors were enzymatically dissociated in digestion buffer (DMEM (Thermo Fisher Scientific, Waltham, MA, USA) containing 0.0625% collagenase (Sigma-Aldrich, St. Louis, MO, USA), 0.125% dispase (Thermo Fisher Scientific) and 2.5% FBS) at 37°C for 60 minutes. Tumors were vigorously agitated by pipetting in PBS, and the tumor fragments were collected and centrifuged at 1000× *g* for 5 minutes. The pellets were suspended in Matrigel (BD Bioscience, Oxford, UK), and 25 μL of this mixture was dispensed in each well. Plates were incubated at 37°C for 10 minutes. The basal medium consisted of Advanced DMEM/F12 (Thermo Fisher Scientific) supplemented with 2 mmol/L of Glutamax, (Thermo Fisher Scientific), 10 mmol/L of HEPES (Sigma-Aldrich), antibiotic antimycotic solution (Sigma-Aldrich), primocin (Thermo Fisher Scientific), B27 supplement (Thermo Fisher Scientific), 1.25 mmol/L of N-acetyl-L-cysteine (Sigma-Aldrich), and 10 nmol/L of gastrin (Sigma-Aldrich). FAP organoids were cultured in ENR medium (basal medium supplemented with ENR (10 ng/mL EGF (Thermo Fisher Scientific), 10% Noggin conditioned medium and 1 μg/mL R-spondin-1 (R&D system, Minneapolis, MN, USA) and were maintained at 37°C at 5% O_2. Media were changed every 3 days.

To prepare Noggin conditioned medium, human Noggin cDNA was cloned into the pFK5K CMV-neo vector (Promega, Fitchburg, MN, USA) and expressed in L1 cells. Transfected cells were selected with 800 μg/mL G418 and were screened with the Dual-Luciferase Assay system (Promega) using BRE-MLP-Luc as a reporter.[7] Conditioned medium was prepared by culturing Noggin-expressing L1 cells in basal medium for 4 days. The activity of these cells was determined using the luciferase assay.

2.2 | Sequence analysis

Organoids were collected in cell recovery solution (Corning, Corning, NY, USA). Genomic DNA was extracted with the QIAamp DNA Mini kit (Qiagen, Valencia, CA, USA), and the DNA quality was analyzed using the Qubit system (Thermo Fisher Scientific). An amount of 200 ng of genomic DNA was used in library construction via the HaloPlex kit (Agilent, Santa Clara, CA, USA), according to the manufacturer's instructions. Target genes were selected based on reported recurrent gene mutations.[8,9] A list of target genes is given in Table S1. Sequencing was performed by on the MiSeq system (Illumina, San Diego, CA, USA). Fastq files were mapped and analyzed using SureCall (Agilent). APC variants were culled by removing those registered in the Human Genetic Variation Database (HGVD release version 2.30). Other variants were annotated with ANNOVAR (2015-03-22 released).[10] The variants were excluded from the following analysis when maximal population frequency is over 1%. We excluded somatic missense SNVs with the following properties; (a) variants were neither deposited on COSMIC (ver82 https://cancer.sanger.ac.uk/cosmic/), (b) any variant fraction of the same patients does not exceed 0.25 (subclonal mutations).

2.3 | Microarray analysis

Organoids were collected in cell recovery solution (Corning), and RNA was extracted using the RNeasy Micro Kit (Qiagen). RNA quality was validated using an Agilent Bioanalyzer. An amount of 100 ng of RNA was used to prepare cRNA using the 3′ IVT PLUS Reagent Kit (Affymetrix, Santa Clara, CA, USA), and the cRNA was hybridized on a U133 Plus 2.0 Array (Affymetrix). GSEA was performed to explore the association of the expression profile of each patient with

the Molecular Signature Database (http://software.broadinstitute.org/gsea/index.jsp). Genes that were differentially expressed (>1.6 fold) between CFAP and AFAP organoids were selected using Gene Spring Software, and the associated signaling pathways were identified using Ingenuity Pathway Analysis (Qiagen).

To investigate chromosomal aberrations, genomic DNA was extracted with the QIAamp DNA Mini Kit (Qiagen), and the quality of the DNA was analyzed on a NanoDrop instrument (Thermo Fisher Scientific). A total of 500 ng of gDNA was hybridized to the Genome-Wide SNP 6 microarray (Affymetrix). CNVs and chromosomal aberrations in the APC gene were identified using Chromosome Analysis Suite (Affymetrix).

2.4 | Viability assay

One day before plating into 384 plates, the media was changed to ENR medium supplemented with 10 μmol/L Y27632 (Sigma). Organoids were digested in TrypLE Express (Thermo Fisher Scientific) supplemented with 10 μmol/L Y27632 at 37°C for 15 minutes with vigorous pipetting every 5 minutes. The cells were suspended in basal medium, and clumps were removed by passing the suspension through a 40 μm cell strainer. The suspension was centrifuged at 1000 g for 5 minutes, and the cells were resuspended in basal medium. This suspension was adjusted to 1.5×10^5 cells/mL in 50% Matrigel in ENR medium, and 2.5 μL of cell suspension was dispensed into each well of 384-well microplates. After polymerization, the cells were cultured for three days in ENR medium supplemented with 10 μmol/L Y27632 and 10 nmol/L PGE2 to form organoids. Cell viability was measured after 3 days of incubation with the drug using the Real-Time-Glo MT Cell Viability Assay (Promega). The data were analyzed using Prism 6 software (Graphpad).

2.5 | Immunoblot analysis

Organoids were collected using a cell recovery solution (Corning) and washed with PBS, and proteins were extracted using 1% NP-40 buffer (20 mmol/L Tris-HCl, pH 8.0, 137 mmol/L NaCl, 1% NP-40, 10% glycerol). The protein concentrations were determined using a protein assay (Bio-Rad, Hercules, CA, USA), and equal amounts of protein were resolved, transferred to nitrocellulose membranes and detected as previously described.[11] The antibodies used for the immunoblot analysis were as follows: anti-STAT1(D1K9Y, Cell Signaling), anti-phosphoSTAT1 (Ser727) (D3B7, Cell Signaling, Danvers, MA, USA), anti-phosphoSTAT1 (Tyr701) (58D6, Cell Signaling), anti-ERK (137F5, Cell Signaling), anti-phosphoERK (Thr202/Tyr204) (D13.14.4E, Cell Signaling), anti-S6 (5G10, Cell Signaling), anti-phosphoS6 (Ser235/236) (D57.2.2E, Cell Signaling), and anti-actin (AC-15, Sigma-Aldrich).

2.6 | Genome editing of FAP organoids

sgRNA-expressing constructs were prepared by cloning a pair of annealed oligonucleotides into the BbsI site of pX330 (Addgene, Watertown, MA, USA). The oligonucleotides were designed based on a 20 bp target sequence (Table S2). One day before electroporation, the media was changed to ENR medium supplemented with 10 μmol/L Y27632 (Sigma). Organoids were digested in TrypLE Express (Thermo Fisher Scientific) supplemented with 10 μmol/L Y27632 at 37°C for 15 minutes with vigorous pipetting every 5 minutes. The cells were suspended in basal medium, and clumps were removed by passing through a 40 μm cell strainer. The suspension was centrifuged at 1000 rpm for 5 minutes, and the cells were resuspended in basal medium. A total of 1×10^6 cells resuspended in 100 μL Opti-MEM (Thermo Fisher Science) were used in electroporation according to the procedure published by Fujii et al.[12] We used 6 μg of each sgRNA-expressing vector, 6 μg of PB-CMV-MCS-EF1-Puro (SBI, Palo Alto, CA, USA) and 1 μg of Super PiggyBac transposase (SBI). After electroporation, the cells were resuspended in 500 μL Opti-MEM supplemented with 10 μg Y27632 at RT for 30 minutes and centrifuged at 1000 rpm for 5 minutes. The cell pellets were resuspended in 200 μL Matrigel, and 25 μL was dispensed in each well of a 48-well plate. The cells were cultured in ENR medium supplemented with 10 μmol/L Y27632 and 10 nmol/L PGE2 for 2 days and subsequently cultured in ENR medium for an additional 3 days. Puromycin selection was started 5 days after electroporation. STAT1 expression was determined by PCR (Table S2) and was confirmed by immunoblot analysis using anti-STAT1 antibody.

2.7 | Genome editing and analysis of mouse intestines

All animal studies and procedures were approved by the JFCR Cancer Institute Animal Care and Welfare Committee. $Apc^{fl/fl}$, Lgr5-CreERT2 mice were generated as previously described.[11] Oocytes were obtained from $Apc^{fl/fl}$, Lgr5-CreERT2 females undergoing superovulation treatment[13] and were used to generate $Apc^{fl/fl}$, Lgr5-CreERT2 embryos using sperm from male $Apc^{fl/fl}$, Lgr5-CreERT2 mice. A pair of oligonucleotides targeting exon 3 of the mouse Stat1 gene (Table S2) was annealed and cloned into the BsaI site of pDR274 (Addgene). The sgRNAs were prepared using the MEGAshortscript T7 Kit (Invitrogen). Amounts of 200 μg/mL sgRNA and 50 ng/mL Cas9 protein (TAKARA, Shiga, Japan) were introduced into the zygotes by electroporation as previously reported.[14] The presence of a 2-bp deletion in exon 3 of STAT1 in founder mice was confirmed by PCR amplification of the targeted region followed by Sanger sequencing, and these mice were used to generate homozygous mutants. Mice carrying wild-type STAT1, which were generated by intercrossing founder mice, were used as controls. Potential off-target sites predicted by Cas-OFFinder (http://www.rgenome.net/cas-offfinder/) were amplified by PCR and analyzed by Sanger sequencing.

To analyze intestinal tumors, the intestine was removed and fixed in 10% neutral formalin (Wako, Tokyo, Japan) for 24 hours, and the Swiss-roll was prepared and embedded in paraffin following recently reported procedures.[15] Four-micron sections were mounted on MAS-coated slides (Matsunami, Tokyo, Japan) and stained with H&E for histological analysis or used for immunohistochemistry. After dewaxing and rehydration via a standard procedure, antigen retrieval was performed either by autoclaving in citrate buffer (pH 6.0) or by using the immunosaver

(Nissin EM, Tokyo, Japan) solution or DAKO Target Retrieval solution, pH 9 (Dako, Tokyo, Japan), according to the manufacturer's instructions. The slides were then incubated overnight at 4°C with primary antibodies. The following antibodies and dilutions were used: mouse anti-beta-catenin (1:10000, Transduction), rabbit anti-STAT1 (1:300, Cell Signaling), rabbit anti-Lysozyme (1:2000, Dako), goat anti-EphB2 (1:2000, R&D), rabbit anti-Cleaved Caspase3 (Asp175) (1:200, Cell Signaling) and rabbit anti-SOX9 (1:1000, Millipore, Burlington, MA, USA). A rabbit anti-EGFP (1:6,500, Abcam, Cambridge, UK) antibody was used as a proxy for Lgr5 expression. The primary antibodies were visualized using the Envision+ system-HRP labeled polymer (Dako) and 3,3′-diaminobenzidine (Vector, Burlingame, CA, USA) according to the manufacturer's instructions. To score the sizes of the adenomatous lesions, images were obtained using an AxioImager M2 microscope (Zeiss), and tiling images were created and scored using the MosaiX and AutoMeasure Modules provided with the AxioVision4 program (Zeiss).

2.8 | Mouse xenograft experiments

Organoids were dissociated into single cells by incubation in TrypLE at 37°C for 15 minutes, and clumps were removed by passing through a 40 μmol/L cell strainer. A total of 1×10^5 cells were resuspended in 50% Matrigel in ENR medium and subcutaneously injected into 6- to 7-week-old female NOD/SCID IL2Rγ^- (NSG) mice using an insulin syringe. The animals were anesthetized with a combination of medetomidine, midazolam and butorphanol.

3 | RESULTS

3.1 | Establishment of FAP organoids

Numerous adenomatous lesions occur in the colorectal region of FAP patients. Each lesion independently arises via the second hit of APC gene as an initiating event and proceeds to tumor development. As a result, these lesions harbor different sets of somatic mutations in an identical genetic background, which supply a valuable resource for genetic and biological analysis. Therefore, we independently cultured organoids derived from surgically resected adenomatous polyps from five FAP patients (Table S3). Three patients, HCT19, 20 and 24, had surgery prior to age 35 and were diagnosed with CFAP, and two patients, HCT14 and 23, underwent surgery after age 60 and were diagnosed with AFAP. Notably, patient HCT24 underwent the first surgery at age of 18 and exhibited the most severe phenotype. Organoids were readily established from both types of FAP tumors, and no significant difference between CFAP and AFAP was noted in the organoid establishment success rate (average 84%) (Table S4). The established organoids were morphologically indistinguishable and contained a clear hollow space lined by a single layer of cells (Figure S1).

The tumor-forming potentials of each organoids were evaluated by subcutaneous transplantation of tumor cells into immune-deficient NOG mice. The organoids were enzymatically dissociated into single cells, and 1×10^5 cells suspended in 50% Matrigel were transplanted into four sites. No tumor formation was evident in 41 out of 42 transplanted FAP organoids, indicating their benign property (Table S3). However, one organoid, HCT24-8, did form a tumor (Table S3). Because all four transplanted grafts developed tumors, HCT24-8 possessed the intrinsic tumor formation potential rather than acquired tumor formation potential during the assay. These observations demonstrated that the FAP organoid set represents various stages ranging from benign tumors to malignant tumors and recapitulates the development of CRC.

3.2 | Genomic characterization of FAP organoids

The genetic aberrations in each organoid were determined via targeted sequence analysis (Figure 1).[8,9] APC alteration was detected in all organoids, and no pathological MUTY mutation was noted, indicating that the organoid sets are derived from APC-associated FAP patients (Figure 1A). The organoids derived from HCT19 and HCT23 harbored common APC mutations of T1821I fs*2 and S89*/T1556N fs*3, respectively. Because the targeted sequence does not detect large deletions, SNP microarray analysis was used to investigate the chromosomal aberrations. Close examinations of the chromosomal region of APC revealed large deletions of 30 kb and 114 kb in HCT14 and HCT24, respectively (Figure 1B). Large deletions encompassing the APC promoter region were previously reported as causative FAP mutations.[16] The S89* mutation in HCT23 and the large deletions in the APC gene in HCT14 were detected in normal blood samples, confirming their germline mutations.

In our analysis, an APC germline mutation was not identified in HCT20. Instead, a mutation in MSH6 was found in this patient, suggesting the possibility that this patient could be affected by HNPCC or Lynch syndrome. It should be noted, however, that the allele frequencies of this mutation were between 0.423 and 0.531, suggesting a heterozygous mutation (Table S5). With regard to the family history of HCT20, her mother and her aunt were diagnosed with FAP-associated colon cancer. As for her previous history, she underwent a total colectomy with ileo-rectal anastomosis because of multiple colon polyps at the age of 32. Follow-up colonoscopy revealed multiple polyps and concomitant early cancer in the residual rectum at the age of 50 (Figure S2A-C). Additional upper gastrointestinal endoscopy showed multiple fundic gland polyps in the stomach (Figure S2D). These clinical features support the FAP diagnosis for HCT20.

Second-hit mutations in the APC gene were identified, four of which were loss-of heterozygosity (LOH) mutations (Figure 1A). Notably, distinct second-hit mutations were detected in each organoid, except for HCT24-10 and -11. Given that second hits in the APC gene occur as an initial event in tumorigenesis, these organoids were thought to arise independently.

It is well established that activation of KRAS is an early event in CRC progression, and in our organoid sets, four organoids harbored the activating mutation of KRAS (Figure 1C). No genetic alterations such as TP53, PIK3CA or SMAD4 were detected, which were believed to occur at a relatively late stage in the tumor progression. Notably, these mutation frequencies were apparently lower than those reported in CRC.[8] These observations further support the notion that FAP organoids represent early events in CRC development.

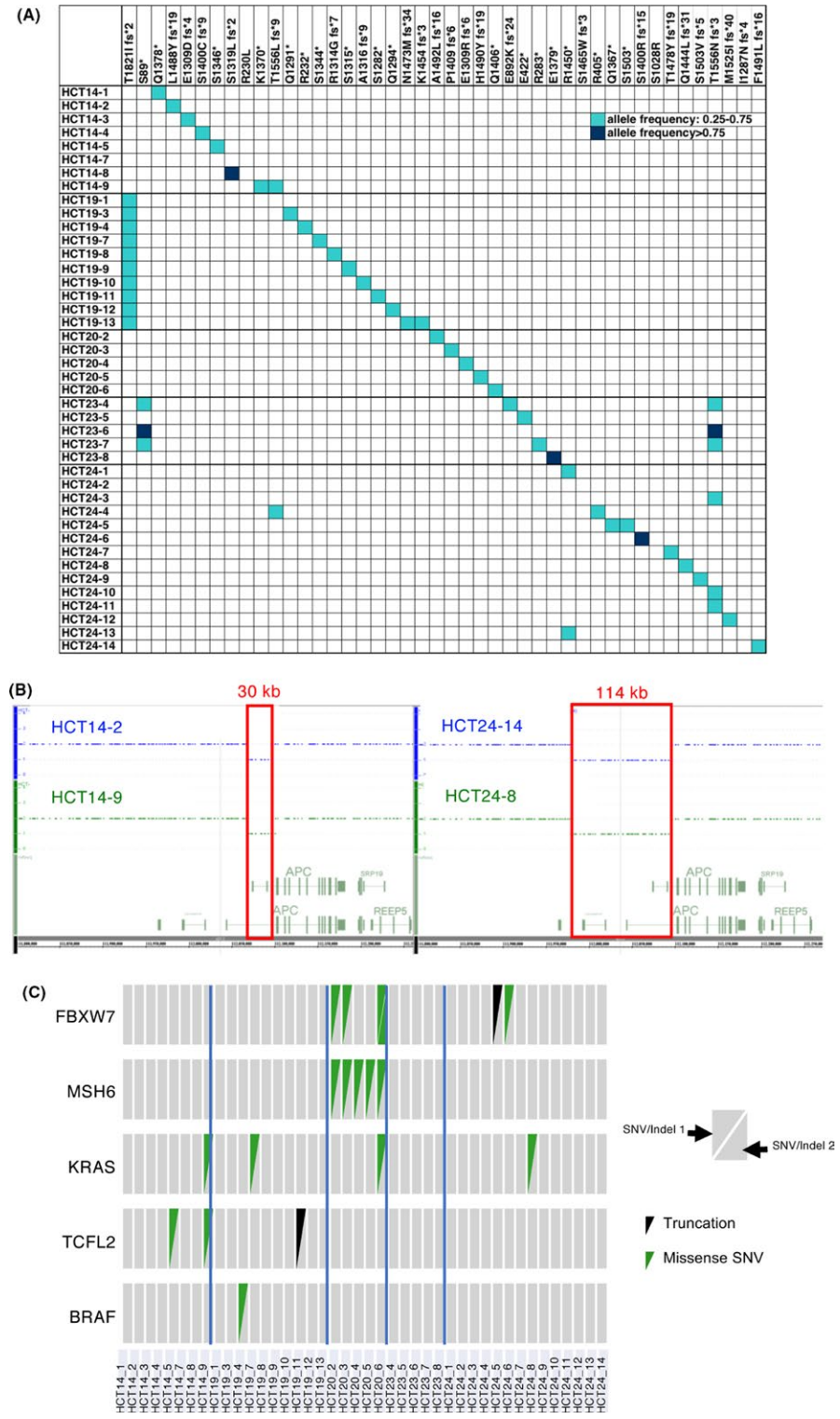

FIGURE 1 Genetic profiling of FAP organoids. (A) Targeted sequence of the APC gene. Allele frequencies are shown as indicated. (B) Large deletion in the promoter region of the APC gene. Chromosome aberrations were analyzed using a SNP6 microarray. Close examination of the APC gene revealed 30 kb and 114 kb deletions encompassing the promoter region in HCT14 and 24, respectively (red box). (C) Somatic and genetic mutations in FAP organoids

3.3 | Inter-patient variations in tumor forming potential

A number of organoids established from the same patients offer us the opportunity to explore the role of the inter-patient genetic variations in tumor formation (Figure 2A). Correlations between clinical manifestations and germline APC mutations have previously been suggested.[17-20] However, in our cohort, these correlations were not observed. For instance, large germline deletions in the promoter region of the APC gene were identified in typical CFAP

(HCT24) and AFAP (HCT14) organoids (Figure 1B). To identify the gene expression patterns associated with the clinical manifestations, we elucidated the characteristic gene expression features of each FAP patients. Interestingly, gene set enrichment analysis (GSEA) of the Molecular Signature Database (MSigDB)[21] revealed that two AFAP organoids, HCT14 and HCT23, were negatively correlated with interferon alpha and gamma response genes, whereas the CFAP organoid HCT24 exhibited a positive correlation with these genes (Figure 2B and Figure S3).

To further clarify the differences, we compared AFAP and CFAP and found striking differences in interferon gamma response (normalized enrichment score (NES) = −1.91, nominal *P*-value (NOM $P < 0.01$), interferon alpha response (NES = −1.88, NOM $P < 0.01$), IL6_JAK_STAT3 signaling (NES = −1.72, NOM $P < 0.01$) and allograft rejection gene sets (NES = −1.69, NOM $P < 0.01$) (Table S6). AFAP was negatively correlated and CFAP was positively correlated with these gene sets (Figure 2C). Furthermore, Ingenuity Pathway Analysis (IPA) identified interferon signaling as the most statistically significant pathway (*Z* score = 3.606, *P* = 1.64E−6) (Figure 2D), supporting the results of GSEA. CFAP organoids exhibited higher expression of the transcription factor STAT1 (2.1-fold) and its target genes, including IFI6 (9.8-fold), IFIT3 (6.6-fold), MX1 (5.7-fold) and ISG15 (2.6-fold) (Figure 2E, Table S7). Taken together, these observations demonstrated a striking association between the IFN/STAT signaling and the clinical features of FAP.

3.4 | Loss of IFN/STAT signaling leads to reduced tumor-forming potentials

The comparative gene expression analysis between CFAP and AFAP demonstrated a correlation between the tumor formation potentials and IFN/STAT signaling. We evaluated the functional relevance using a mouse model of FAP. The sgRNAs were designed to target exon3 of Stat1, and genome editing was conducted in zygotes carrying a homozygous conditional Apc allele ($Apc^{fl/fl}$) and an Lgr5-CreERT2 allele (Figure 3A). We obtained mutant mice carrying bi-allelic 2 bp deletions ($Stat1^{null/null}$), and this deletion led to a frame-shift following the N-terminal 26 amino acids (Figure S4). No off-target mutations were detected (Table S8). Stat1 was highly expressed in intestinal tumors induced via disruption of the Apc gene, whereas $Stat1^{null/null}$ mice completely lost Stat1 expression, confirming the bi-allelic disruption of the Stat1 gene (Figure 3B). Importantly, the tumor area, determined by scoring β-catenin accumulation (Figure S5), was significantly reduced in the intestines of Stat1-deficient animals (N = 6, $P < 0.01$, *t*-test) (Figure 3C). Lgr5 was strongly expressed in the lower regions and gradually decreased toward the upper domain of the lesion (Figure S6), indicating stem cell expansion in response to Apc inactivation. Stat1 disruption did not alter the cellular composition of the lesion or the frequency of apoptosis, but it reduced the number of both Lgr5-positive and Lgr5-negative cycling cells (27.8% vs. 20.8%, $P < 0.05$, and 43.6% vs. 34.2%, $P < 0.01$, *t*-test, respectively) (Figure 3D and E). These observations demonstrated the functional relevance of IFN/STAT signaling in the clinical features of FAP patients.

3.5 | IFN/STAT signaling is elevated in RAS-activated organoids

HCT24 exhibited high IFN/STAT signaling activity, and HCT24-8 harboring the KRAS mutation formed xenograft tumors in immunodeficient mice. To gain insights into the role of KRAS mutation in tumor-formation potential, the gene expression of HCT24-8 was compared with that derived from the same patients (Figure 4A, top row). GSEA identified 24 gene sets that were significantly enriched, including hedgehog signaling (NES = 2.11 NOM $P < 0.01$), epithelial mesenchymal transition (NES = 2.05, NOM $P < 0.01$) and KRAS signaling (NES = 1.81, NOM $P < 0.01$). Notably, two IFN/STAT signaling-related gene sets were enhanced, namely, interferon alpha response and interferon gamma response. The NES and NOM p-values of HCT24-8 in interferon alpha and gamma were 1.67 and 0.000 and 1.53 and 0.000, respectively (Figure 4B). The elevated IFN/STAT signaling related gene sets were also observed in HCT14-9, HCT19-7 and HCT20-6, which harbored activating mutations of KRAS (Figure 4A). These observations suggested that the activating mutations of KRAS enhanced IFN/STAT signaling in FAP organoids.

To gain mechanical insights into the crosstalk between RAS signaling and IFN/STAT signaling, phosphorylation of the STAT1 protein was examined. Immunoblot analysis showed significant increases in phosphorylated ERK and S6, confirming the activation of RAS signaling in HCT24-8 and HCT24-8x, which was established from the xenograft tumor (Figure 4C). STAT family proteins are activated through Janus kinase (JAK)-mediated tyrosine phosphorylation.[22] However, phosphorylation of Tyr701 was minimally detected in these organoids. Instead, we observed elevated phosphorylation at Ser727, which is mediated by the ERK family of protein kinases.[23,24] Similar observations were made in HCT19-7, which was derived from a CFAP patient and harbored a KRAS mutation (Figure S7).

Interestingly, immunohistochemical analysis revealed that STAT1 was highly expressed in the HCT24-8 xenograft tumor, and phosphorylation of Ser727 but not Tyr701 was detected (Figure 4D, Figure S8). Furthermore, STAT1 protein phosphorylate at Ser727 was accumulated in the nucleus. These observations support the notion that the activating mutation of KRAS enhanced IFN/STAT signaling by phosphorylation of the STAT1 protein.

3.6 | IFN/STAT signaling confers resistance to MEK inhibitors in KRAS mutant organoids

The analysis described above suggested that IFN/STAT signaling stimulated cell proliferation as a downstream target of RAS. We tested this hypothesis using chemotherapeutic agents targeting RAS signaling. As expected, the EGFR inhibitor gefitinib effectively reduced the viability of FAP organoids, but the activating mutation of KRAS conferred resistance (Figure 5A). In contrast, downstream perturbation of RAS by the MEK inhibitor trametinib reduced the viability of organoids harboring KRAS mutations (HCT14-9 and HCT20-6) (Figure 5B). However, unexpectedly, two other KRAS-mutated organoids, HCT19-7 and HCT24-8, were resistant to

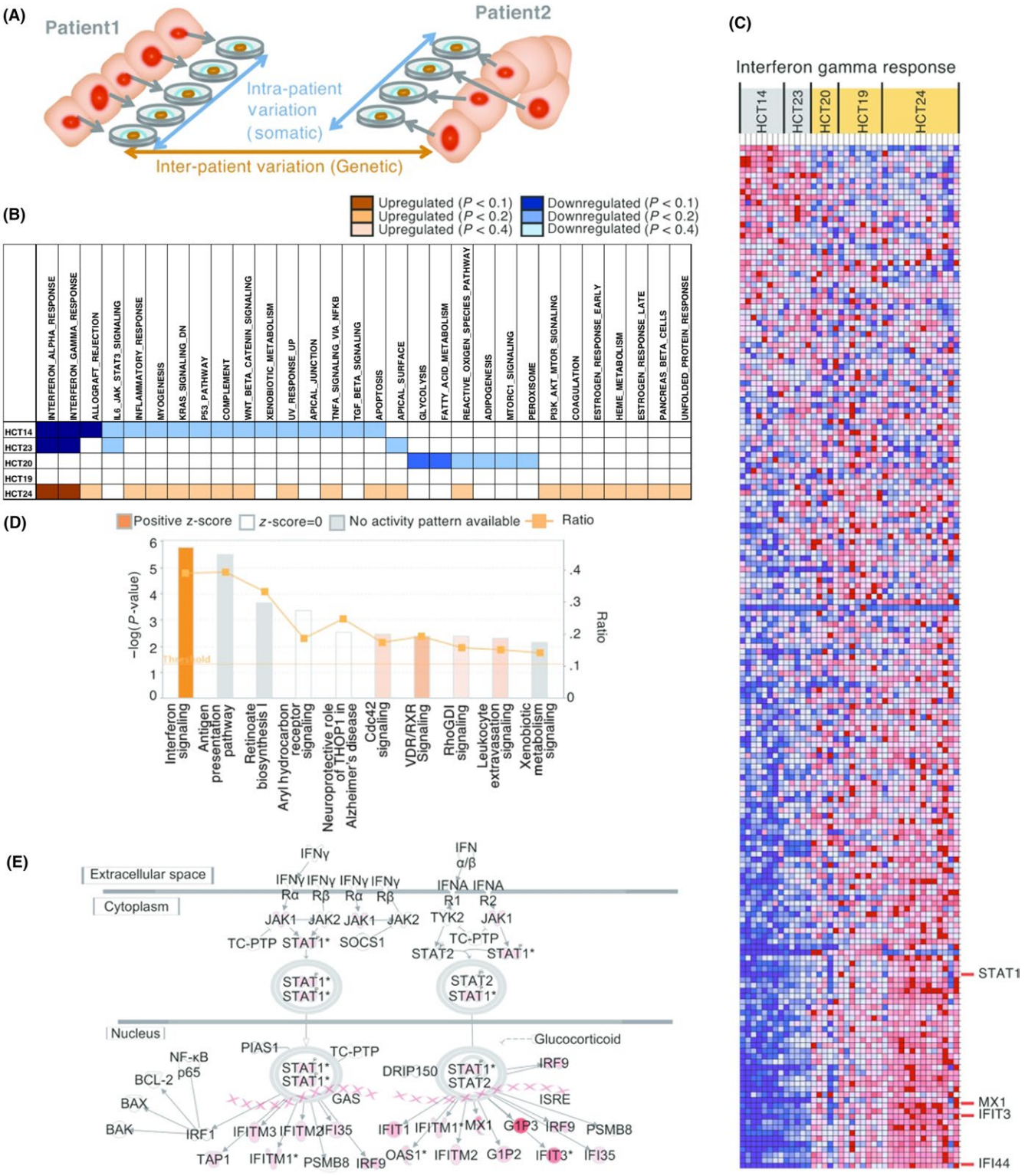

FIGURE 2 FAP organoid gene expression analysis. (A) To elucidate the expression profiles associated with inter-patient variations, patient data sets were compared. (B) Individual patient expression data were tested against data from all other patients using the gene set analysis tool from the Molecular Signature Database. HCT14 and 23 were negatively correlated with Interferon alpha gamma response genes, and HCT24 demonstrated a positive correlation with these genes. (C) Heatmap showing a comparative analysis between CFAP (HCT19, 20 and 24) and AFAP (HCT14 and 23) samples. (D) Pathway-based IPA analysis identified interferon signaling as the most closely relevant signaling pathway. (E) Interferon signaling gene expression analysis. Genes expressed >1.6-fold more highly in CFAP compared with AFAP are shown in light red, and those expressed >5-fold more highly are shown in dark red

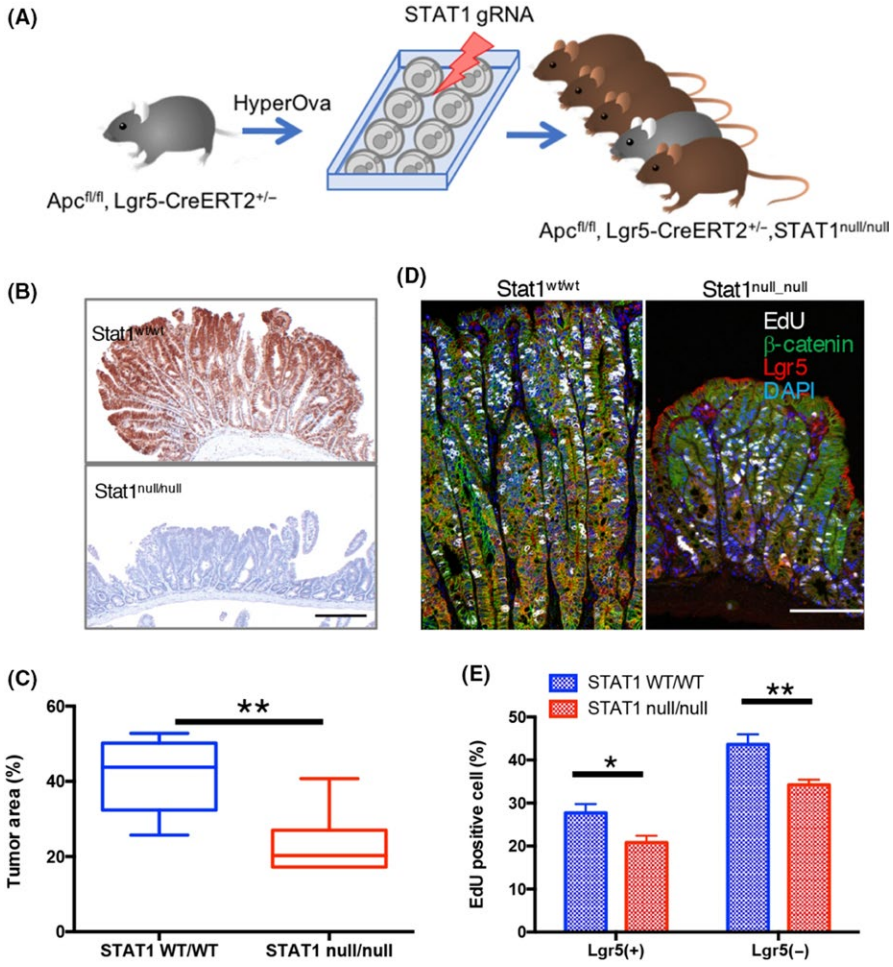

FIGURE 3 Disruption of Stat1 in a mouse model of FAP. (A) Stat1-deficient mice were generated by introducing Stat1 sgRNA into zygotes carrying the $Apc^{fl/fl}$, Lgr5-CreERT2$^{+/-}$ allele. (B) Immunohistochemical analysis of intestinal tumors. $Apc^{fl/fl}$, Lgr5-CreERT2, $Stat1^{wt/wt}$ ($Stat1^{wt/wt}$) or $Apc^{fl/fl}$, Lgr5-CreERT2, $Stat1^{null/null}$ ($Stat1^{null/null}$) mice were analyzed 26 days after administration of 4OHT. Immunohistochemical analysis is shown using an anti-Stat1 antibody. Bar = 200 μm. (C) Disruption of Stat1 suppresses tumor formation. Tumors in the indicated mice (N = 6) were detected by immunohistochemistry using an anti-β-catenin antibody, and the tumor area was measured. $^{**}P < 0.01$, unpaired *t*-test. (D) Reduction of cycling cells in Stat1-deficient tumor. Cycling cells were detected by EdU and are shown in white. Tumor cells (detected by β-catenin) and stem-like cells (detected by EGFP) are shown in green and red, respectively. Nuclei were stained with DAPI (blue). Bar = 100 μm. (E) Quantification of cycling cells. Lgr5-positive and Lgr5-negative cycling cells were counted in the indicated mice (N = 6). $^{*}P < 0.05$, $^{**}P < 0.01$

trametinib treatment. Similar results were obtained using another MEK inhibitor (selumetinib), confirming that these organoids were resistant to inhibition of MEK activity (Figure S9).

We examined whether trametinib inhibited RAS signaling in resistant organoids because accumulating evidence indicates that cancer cells acquire resistance to MEK inhibitors through persistent RAS signaling.[25-27] However, trametinib efficiently inhibited phosphorylation of ERK in HCT24-8 and -8x, and no persistent RAS signaling was observed (Figure S10). We next focused on the correlation between sensitivity to MEK inhibitors and the IFN/STAT signaling because the two resistant clones were derived from CFAP and the sensitive clones were derived from AFAP. Since organoids derived from CFAP expressed higher STAT1 levels than those derived from AFAP and since unphosphorylated STAT1 has been reported to transduce the signaling,[28] this correlation raised the possibility that high STAT1 expression conferred the resistance to MEK inhibitors. To test this hypothesis, we disrupted STAT1 in HCT24-8 and examined the change in the response to MEK inhibitors. Using the CRISPR/Cas9 system, we obtained HCT24-8-STAT1KO cells harboring a bi-allelic 38 bp deletion, which resulted in a frame shift after the N-terminal 15 amino acids (Figure S11A).[12] Complete loss of STAT1 protein was confirmed by immunofluorescence analysis and immunoblot analysis (Figure 6A, Figure S11B and C). As expected, GSEA analysis identified Interferon alpha and gamma response as the gene sets most correlated with the STAT1 disruption (NES = 1.76, NOM $P < 0.001$ and NES = 1.48, NOM $P = 0.004$, respectively) (Figure 6B and Table S9). We examined the drug response of HCT24-8 STAT1KO and found that disruption of STAT1 did not affect the response to gefitinib but significantly restored the sensitivity to trametinib (Figure 6C). Immunoblot analysis revealed that disruption of STAT1 did not affect the inhibition of ERK phosphorylation by MEK inhibitors, indicating that the effect of STAT1 disruption was independent of ERK activity (Figure S12). Taken together, these observations demonstrated that high intrinsic IFN/STAT signaling activity confers resistance to MEK inhibitors in RAS-activated FAP organoids (Figure 6D).

4 | DISCUSSION

FAP is an autosomal dominant inherited disease caused by germline mutation of APC gene. In this study, we established 42 organoids from five patients. Genomic sequence analysis of the APC gene identified germline mutations and somatic mutations, confirming the model proposed for the adenoma formation in FAP patients. Activating mutations of KRAS, which are considered as the early event in CRC progression, were detected, but the frequencies were

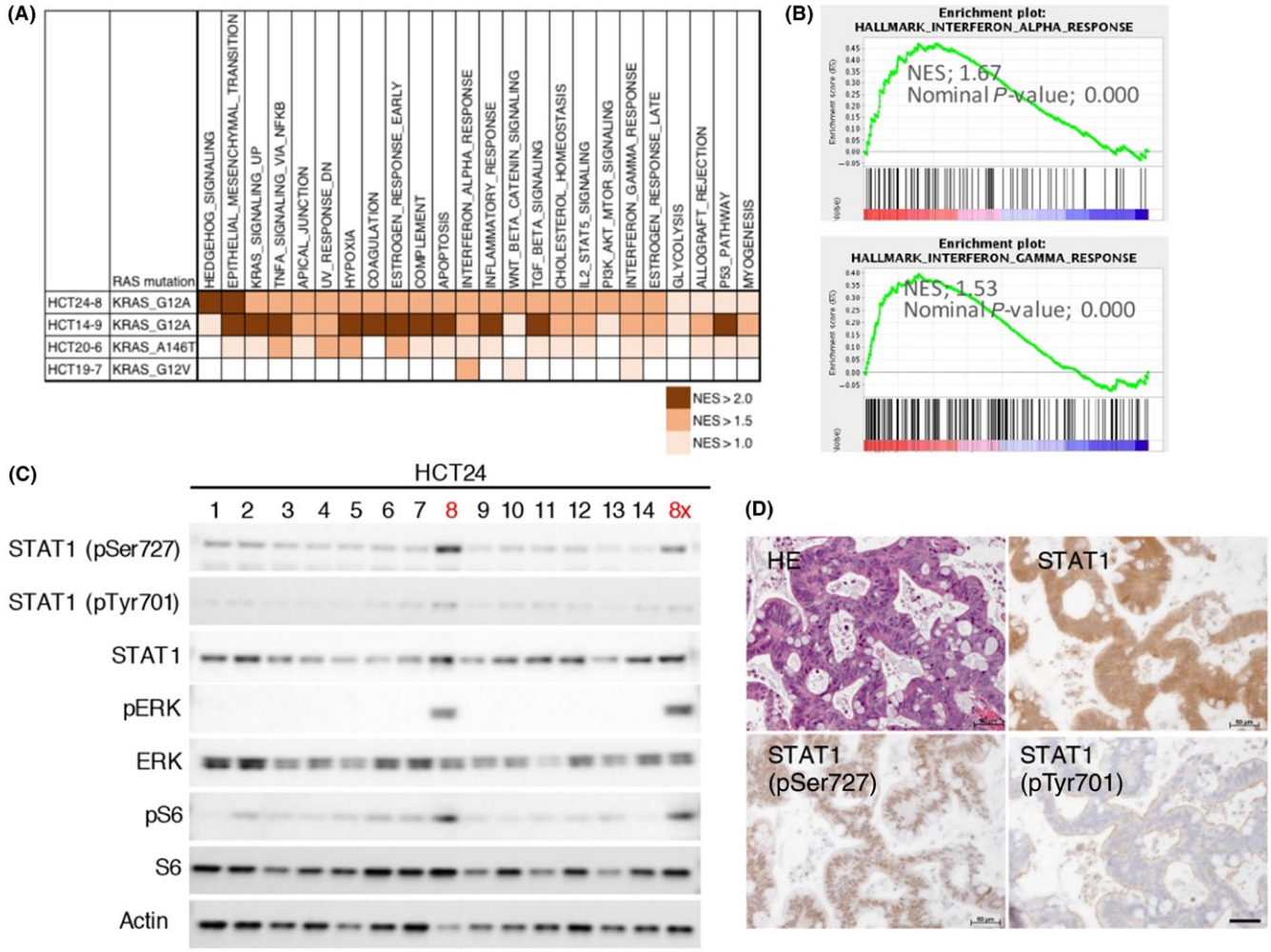

FIGURE 4 Crosstalk between RAS and IFN/STAT signaling. (A) GSEA of FAP organoids. The expression profile of an organoid harboring the KRAS mutation was compared with those of the remaining organoids derived from the same patient. (B) Enrichment plots of HCT24-8. Interferon alpha and gamma responses are shown. (C) Immunoblot analysis of organoids derived from HCT24. (D) Histological analysis of the xenograft tumor derived from HCT24-8. The results of HE staining and immunohistochemistry using the indicated antibodies are shown

lower than those reported in sporadic CRC.[8] Similarly, pathogenic mutations in driver genes including TP53, SMAD4, PIK3CA and BRAF were rarely detected. Notably, 41 out of 42 organoids failed to grow in immune-deficient mice, indicating their benign property. These observations demonstrated that the genetic features and biological properties of the FAP organoid panel established in this study reproduced the early process in CRC development.

Based on severity, FAP patients were classified into two major subtypes. Correlations between the clinical manifestations and the germline mutations of APC gene have been suggested, and the current model indicated that AFAP is associated with mutations in the 5′ end of APC gene within exon9 or at the 3′ distal end of the gene.[17,18] More recently, large inron14 rearrangement[19] and point mutations at the first 15-AA repeats have been shown to be associated with AFAP.[20] However, in our cohort, these phenotype-genotype correlations were not observed, and thus the germline mutations alone cannot fully explain the phenotypic difference. Instead, we found that the activity of IFN/STAT signaling was tightly correlated with the phenotype. Importantly, Stat1 inactivation in the mouse model of FAP suppressed tumor formation, indicating its biological relevance. These observations suggested that the IFN/STAT signaling is a novel factor regulating the clinical manifestations of FAP patients. We identified STAT1 as one of the causes of the inter-patient variations of IFN/STAT signaling. Exploring the regulation of STAT1 expression and searching for other molecules controlling IFN/STAT signaling could be of particular interest.

Traditionally, IFN/STAT signaling has been connected to anti-tumorigenic effects by regulation of caspases, cyclin-dependent kinase inhibitor and the IRF1/p53 pathway. However, depending on the cellular context, IFN/STAT signaling has been shown to mediate tumor cell growth, metastasis and chemo- and radio-resistance.[29] In this study, using the conditional Apc knockout mice and Lgr5-CreERT2 mice, we have shown the critical roles of IFN/STAT signaling in the tumor formation potential of APC-deficient intestinal cells. A previous study using conventional Apc-knockout mice, Apc^{min}, indicated that Stat1 disruption did not affect the polyp number or

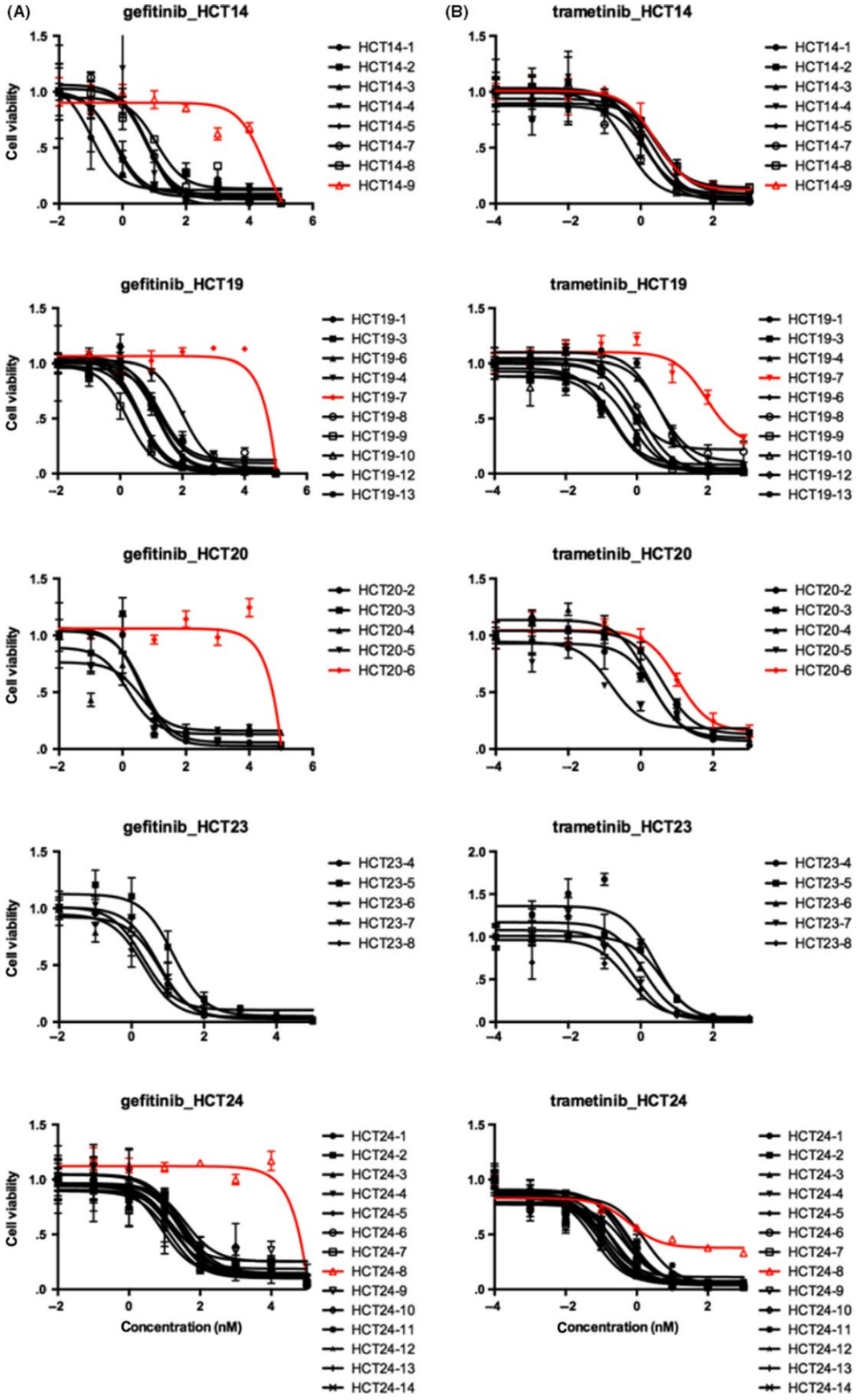

FIGURE 5 Response of FAP organoids to RAS signaling inhibitors. Response to gefitinib (A) and trametinib (B). Organoids harboring activating KRAS mutations are shown in red

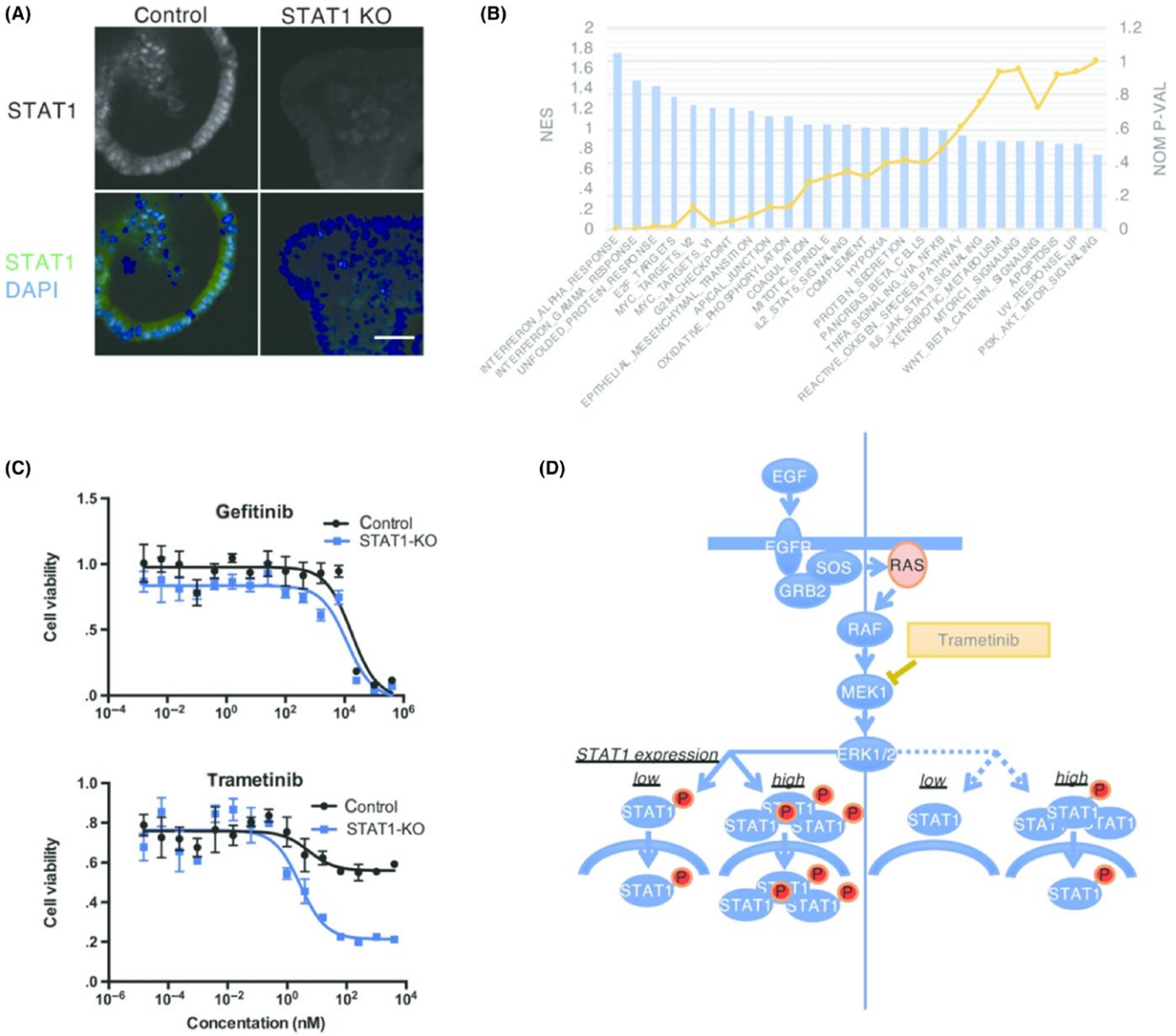

FIGURE 6 STAT1 disruption sensitized KRAS-activated organoids to trametinib. (A) Disruption of STAT1. STAT1 knockout and control organoids were stained with anti STAT1 antibody. (B). GSEA of STAT1 KO organoids. NES (bar graph) and nominal *P*-value (line graph) are shown. (C) Response of STAT1-deficient organoids. STAT1 KO (blue line) and control (black line) are shown. (D) Schematic representation of crosstalk between RAS signaling and IFN/STAT signaling. The phosphorylation status of STAT1 with (right side) or without (left side) trametinib treatment is illustrated. Activated RAS induces STAT1 phosphorylation and activates IFN/STAT signaling. Trametinib inhibits MEK activity, but does not abolish STAT1 phosphorylation, which confers resistance in CFAP organoids

distribution.[30] This discrepancy may indicate that Stat1 plays specific roles in stem-cell expansion, as we used Lgr5-CRE^{ERT2} to disrupt the Apc gene to make a specific disruption in crypt base columnar cells. Alternatively, the phenotype could be due to allele differences, as the armadillo repeats were retained in the Apc^{min} allele, while they were disrupted in the Apc^{580D} allele, which was generated from the Apc$^{fl/fl}$ allele following Cre recombinase activation. Phenotypic differences among mutant alleles of the human APC gene have been reported.[17] The role of IFN/STAT signaling in APC-deficient cells has been genetically shown in the *Drosophila* adult midgut system.[31] Loss of Apc1 leads to hyperproliferation of intestinal stem cells, and knockdown of STAT-mediated signaling suppresses hyperproliferation of Apc1-deficient intestinal stem cells. The role of IFN/STAT signaling in the expansion of Apc-deficient progenitor cells was also demonstrated in zebrafish.[32] Moreover, the crosstalk of RAS signaling and IFN/STAT signaling in APC-deficient intestinal cells was shown in the genetic models of *Drosophila* and mouse.[33] These results support our conclusion that IFN/STAT signaling enhances the tumor-forming potential of APC-deficient intestinal cells and point to its evolutionally conserved mechanisms.

We found that enhanced IFN/STAT signaling confers trametinib resistance in CFAP organoids harboring a KRAS mutation. It should be

noted that a difference between CFAP and AFAP was not observed in those carrying wild-type KRAS (Figure 5), suggesting that activated KRAS plays roles in trametinib sensitivity (Figure 6D). We have noticed that the phosphorylation of Ser724 of STAT1 in KRAS-activated organoid was not inhibited by trametinib (Figure S13), suggesting that other kinases compensate for MEK activity. Several kinases, including mTOR, PKC and p38, have been reported to phosphorylate Ser727 of STAT1. Since these kinases are controlled, at least in part, by RAS, but are independent of MEK activity, they can potentiate trametinib resistance in CFAP organoids.[23] Alternatively, indirect crosstalk between the RAS and IFN/STAT signaling pathways may contribute to the differences in trametinib sensitivity between CFAP and AFAP. For instance, RAS phosphorylates BAD to control IFN/STAT-mediated apoptosis.[34] Further investigation is needed to gain mechanistic insight into the differences in trametinib sensitivity.

In this study, we have found that IFN/STAT singling enhances the tumor-forming potentials of APC-deficient intestinal cells. These findings might shed light on potential therapeutic strategies for CFAP patients that could suppress tumor formation to rates more similar to those found in AFAP. The ability to delay total coloproctectomy could be beneficial for CFAP patients because this procedure inevitably worsens the postoperative quality of life. Suppression of IFN/STAT signaling might accomplish follow-up without surgical intervention. We also have demonstrated that inter-patient variations in IFN/STAT signaling determine the response to MEK inhibitors. RAS signaling is one of the most potent targets for cancer therapy. In CRC, EGFR inhibitors are currently in clinical use in treatment of patients with RAS-wild status. Extensive efforts have been made to develop MEK inhibitors for tumors harboring mutant RAS,[35] but clinical trials thus far showed only modest efficacy with a single agent or combinations.[36] Our findings might offer a rationale for the stratification of patients and for the development of combination therapies including both MEK inhibitors and agents that perturb IFN/STAT signaling.

ACKNOWLEDGMENTS

We would like to thank T. Sato (Keio University) for the kind advice on organoid culture and P. ten Dijke (Ludwig Institute for Cancer Research) and D. Koinuma (University of Tokyo) for the BRE-MLP-Luc plasmid. We are grateful to S. Amino and Y. Ota (Japanese Foundation for Cancer Research) for performing the microarray experiments. This work was supported in part by MEXT/JSPS KAKENHI grant numbers 16H06276-1 (R. Yao), 16K14620 (R.Yao), 17H063333 (R. Yao) and 18H02684 (R. Yao), and a grant from the Vehicle Racing Commemorative Foundation (R. Yao).

CONFLICT OF INTEREST

The authors have no conflict of interest to declare.

ORCID

Ryoji Yao https://orcid.org/0000-0003-0327-0965

REFERENCES

1. Vogelstein B, Papadopoulos N, Velculescu VE, Zhou S, Diaz LA Jr, Kinzler KW. Cancer genome landscapes. *Science*. 2013;339:1546-1558.
2. Drost J, van Jaarsveld RH, Ponsioen B, et al. Sequential cancer mutations in cultured human intestinal stem cells. *Nature*. 2015;521:43-47.
3. Matano M, Date S, Shimokawa M, et al. Modeling colorectal cancer using CRISPR-Cas9-mediated engineering of human intestinal organoids. *Nat Med*. 2015;21:256-262.
4. Nishisho I, Nakamura Y, Miyoshi Y, et al. Mutations of chromosome 5q21 genes in FAP and colorectal cancer patients. *Science*. 1991;253:665-669.
5. Nielsen M, Bik E, Hes FJ, et al. Genotype-phenotype correlations in 19 Dutch cases with APC gene deletions and a literature review. *Eur J Hum Genet*. 2007;15:1034-1042.
6. Nagase H, Miyoshi Y, Horii A, et al. Correlation between the location of germ-line mutations in the APC gene and the number of colorectal polyps in familial adenomatous polyposis patients. *Cancer Res*. 1992;52:4055-4057.
7. Korchynskyi O, ten Dijke P. Identification and functional characterization of distinct critically important bone morphogenetic protein-specific response elements in the Id1 promoter. *J Biol Chem*. 2002;277:4883-4891.
8. Cancer Genome Atlas N. Comprehensive molecular characterization of human colon and rectal cancer. *Nature*. 2012;487:330-337.
9. Kandoth C, McLellan MD, Vandin F, et al. Mutational landscape and significance across 12 major cancer types. *Nature*. 2013;502:333-339.
10. Wang K, Li M, Hakonarson H. ANNOVAR: functional annotation of genetic variants from high-throughput sequencing data. *Nucleic Acids Res*. 2010;38:e164.
11. Yao R, Oyanagi J, Natsume Y, et al. Suppression of intestinal tumors by targeting the mitotic spindle of intestinal stem cells. *Oncogene*. 2016;35:6109-6119.
12. Fujii M, Matano M, Nanki K, Sato T. Efficient genetic engineering of human intestinal organoids using electroporation. *Nat Protoc*. 2015;10:1474-1485.
13. Takeo T, Nakagata N. Superovulation using the combined administration of inhibin antiserum and equine chorionic gonadotropin increases the number of ovulated oocytes in C57BL/6 female mice. *PLoS One*. 2015;10:e0128330.
14. Hashimoto M, Yamashita Y, Takemoto T. Electroporation of Cas9 protein/sgRNA into early pronuclear zygotes generates non-mosaic mutants in the mouse. *Dev Biol*. 2016;418:1-9.
15. Bialkowska AB, Ghaleb AM, Nandan MO, Yang VW. Improved Swiss-rolling Technique for Intestinal Tissue Preparation for Immunohistochemical and Immunofluorescent Analyses. *J Vis Exp*. 2016;113:e54161.
16. Rohlin A, Engwall Y, Fritzell K, et al. Inactivation of promoter 1B of APC causes partial gene silencing: evidence for a significant role of the promoter in regulation and causative of familial adenomatous polyposis. *Oncogene*. 2011;30:4977-4989.
17. Soravia C, Berk T, Madlensky L, et al. Genotype-phenotype correlations in attenuated adenomatous polyposis coli. *Am J Hum Genet*. 1998;62:1290-1301.
18. Spirio L, Otterud B, Stauffer D, et al. Linkage of a variant or attenuated form of adenomatous polyposis coli to the adenomatous polyposis coli (APC) locus. *Am J Hum Genet*. 1992;51:92-100.
19. Tuohy TM, Done MW, Lewandowski MS, et al. Large intron 14 rearrangement in APC results in splice defect and attenuated FAP. *Hum Genet*. 2010;127:359-369.

20. Menendez M, Gonzalez S, Obrador-Hevia A, et al. Functional characterization of the novel APC N1026S variant associated with attenuated familial adenomatous polyposis. *Gastroenterology*. 2008;134:56-64.
21. Liberzon A, Subramanian A, Pinchback R, Thorvaldsdottir H, Tamayo P, Mesirov JP. Molecular signatures database (MSigDB) 3.0. *Bioinformatics*. 2011;27:1739-1740.
22. Ivashkiv LB, Donlin LT. Regulation of type I interferon responses. *Nat Rev Immunol*. 2014;14:36-49.
23. Decker T, Kovarik P. Serine phosphorylation of STATs. *Oncogene*. 2000;19:2628-2637.
24. Wen Z, Zhong Z, Darnell JE Jr. Maximal activation of transcription by Stat1 and Stat3 requires both tyrosine and serine phosphorylation. *Cell*. 1995;82:241-250.
25. Poulikakos PI, Solit DB. Resistance to MEK inhibitors: should we co-target upstream? *Sci Signal*. 2011;4:pe16.
26. Manchado E, Weissmueller S, Morris JPt, et al. A combinatorial strategy for treating KRAS-mutant lung cancer. *Nature*. 2016;534:647-651.
27. Sun C, Hobor S, Bertotti A, et al. Intrinsic resistance to MEK inhibition in KRAS mutant lung and colon cancer through transcriptional induction of ERBB3. *Cell Rep*. 2014;7:86-93.
28. Yang J, Stark GR. Roles of unphosphorylated STATs in signaling. *Cell Res*. 2008;18:443-451.
29. Khodarev NN, Roach P, Pitroda SP, et al. STAT1 pathway mediates amplification of metastatic potential and resistance to therapy. *PLoS One*. 2009;4:e5821.
30. Liddle FJ, Frank DA. STAT1 expression is not required for polyp formation in Min mice. *Mol Carcinog*. 2008;47:75-79.
31. Cordero JB, Stefanatos RK, Myant K, Vidal M, Sansom OJ. Non-autonomous crosstalk between the Jak/Stat and Egfr pathways mediates Apc1-driven intestinal stem cell hyperplasia in the Drosophila adult midgut. *Development*. 2012;139:4524-4535.
32. Lin J, Wang X, Dorsky RI. Progenitor expansion in apc mutants is mediated by Jak/Stat signaling. *BMC Dev Biol*. 2011;11:73.
33. Cordero JB, Ridgway RA, Valeri N, et al. c-Src drives intestinal regeneration and transformation. *EMBO J*. 2014;33:1474-1491.
34. Winter PS, Sarosiek KA, Lin KH, et al. RAS signaling promotes resistance to JAK inhibitors by suppressing BAD-mediated apoptosis. *Sci Signal*. 2014;7:ra122.
35. Samatar AA, Poulikakos PI. Targeting RAS-ERK signalling in cancer: promises and challenges. *Nat Rev Drug Discov*. 2014;13:928-942.
36. Janne PA, Shaw AT, Pereira JR, et al. Selumetinib plus docetaxel for KRAS-mutant advanced non-small-cell lung cancer: a randomised, multicentre, placebo-controlled, phase 2 study. *Lancet Oncol*. 2013;14:38-47.

SUPPORTING INFORMATION

Additional supporting information may be found online in the Supporting Information section at the end of the article.

How to cite this article: Sakahara M, Okamoto T, Oyanagi J, et al. IFN/STAT signaling controls tumorigenesis and the drug response in colorectal cancer. *Cancer Sci*. 2019;110:1293–1305. https://doi.org/10.1111/cas.13964